Digital Control of a Fast Field Cycling NMR Relaxometer Power Supply

Rúben J. A. Lopes
Under Supervision of Prof. Pedro José Oliveira Sebastião and Prof. Duarte de Mesquita e Sousa
Mestrado Integrado em Engenharia Física Tecnológica
Instituto Superior Técnico, Lisboa, Portugal

(Dated: April 2014)

Fast Field Cycling (FFC) Nuclear Magnetic Resonance (NMR) is a powerful technique that allows to overcome a technical difficulty associated to low frequency spin-lattice relaxation measurements using conventional NMR spectrometers. This difficulty is related to the NMR signal-to-noise ratio (SNR) that decreases with the magnetic field. In a FFC-NMR experiment to measure the spin-lattice relaxation time the sample is submitted to different *Zeeman* fields at different times, allowing measurement of the magnetization decay with time at a low magnetic field, but detecting the NMR signal when the sample is submitted to a magnetic field which provides good SNR measuring conditions.

In this dissertation, a digital control system for a FFC-NMR relaxometer power supply was developed. The hardware and software were designed to allow for the modulation of the *Zeeman* field as required by this technique. Experimental results show that under digital control the system performs fast transitions between the high and low magnetic field and assures a good stability of the field during the steady states. The switching times obtained are in the millisecond range. Comparative proton relaxometry measurements in two compounds (liquid crystal 5CB and ionic liquid [BMIM]BF4) were made to assess the digital control system performance.

Keywords: Nuclear Magnetic Resonance, NMR Relaxometer, Fast Field Cycling NMR, Digitally Controlled Power Supply, Digital Control System, Microcontroller

INTRODUCTION

Nuclear Magnetic Ressonance (NMR) spectroscopy is a technique that exploits magnetic properties of atomic nucleus. This system is able to dissipate the absorbed energy and to relax to equilibrium with a characteristic time that depends on the molecular structure and local molecular order. Variations on these characteristic times are the subject of studies in organic compounds like Ionic Liquids and Liquid Crystals. [1] The main purpose of this technique is to study molecular order and dynamics in different materials, using the nuclear spins and their interactions as a probing system.

There are different NMR techniques used to study molecular dynamics by measuring relaxation times T_1 *spin-lattice* and T_2 *spin-spin*. These quantities characterize the evolution of the nuclear magnetization towards the equilibrium. The main difficulty associated to the NMR relaxometry at different magnetic fields is the SNR of the measured NMR signal. NMR SNR decreases with the magnetic field. [2][3]. Therefore, conventional NMRs spectrometers, which operate at fields above 0.1 T, are not suitable to perform studies of resonance frequencies associated to low magnetic fields. [4]

Fast Field Cycling NMR (FFC-NMR) is a technique used to overcome this difficulty, by applying different magnetic fields at distinct times, but always measuring the NMR induction signal when the sample is submitted to a high magnetic field. In general, the magnetic field varies cyclically as it's illustrated in Figure 1.

At first, the sample is placed in a strong magnetic field B_{0P} for polarization. Following this, the magnetic field is switched down to a lower value B_{0E} that is applied during a time t_E. Next, the field is switched up to a stronger magnetic field B_{0D} and finally the magnetic field is switched back to the initial value B_{0P}. Since the detection of the NMR signal is made when the sample is submitted to B_{0D}, which is larger than B_{0E}, the sensitivity of the quality of the NMR signal detected is independent of the evolution occurring during t_E. [3] [5]

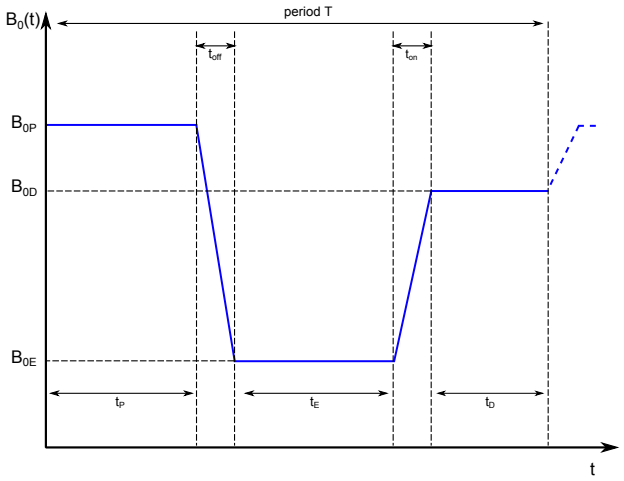

Figure 1: Time diagram of the FFC-NMR spectroscopy technique.

Figure 2 shows the typical configuration of a NMR spectrometer. [3] [2]

In order to implement the cycle represented in Figure 1, the current supplied to the magnet coils that produce the magnetic field $\vec{B_0}$ must be controlled in such a way that the transitions between the different magnetic fields are fast, but the field is stable during the steady states. This means that the power supply of a FFC-NMR spectrometer requires a control system that guarantees steady and stable currents during t_p, t_e and t_d and regulated transitions of the current between these steady periods of the cycle.

This project aims at the implementation of a digital control system to be used in a pre-production NMR re-

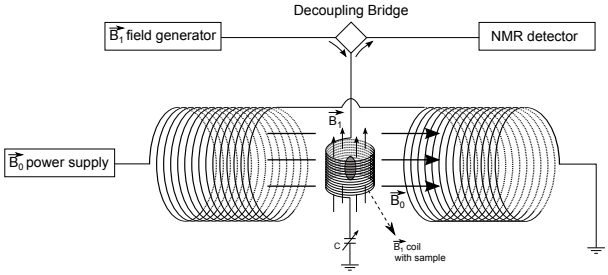

Figure 2: Block diagram of a typical configuration of a NMR spectrometer.

laxometer prototype under development. This embedded system is going to replace part of the analog technology currently used in the power supply control system.

STATE OF THE ART

Fast Field Cycling Nuclear Magnetic Resonance has long been proven to be a powerful technique with applications in molecular dynamic studies. [6] [5] Cycling the magnetic field using mechanical systems was the earliest form of field cycling relaxometry. In these systems the sample was mechanically shuttled between two positions and submitted to different magnetic fields. This is a simple way to obtain a $\boldsymbol{B}_0$ cycle by transporting the sample between two magnets (several references in [3]).

However, shuttling the sample mechanically (using air pressure) involved switching times in the order of 100's of ms, limiting this methodology to measurements of longer relaxation times only.

In modern NMR relaxometers the magnetic field is switched by between levels using sophisticated power supplies that use power semiconductors to control the electric current flowing in the magnet's coils. Even though a rather more complex apparatus is used in this solution, faster switching is possible, allowing a greater diversity of possible experiments. Electronically switched field-cycling instruments have been able to switch high magnetic inductions with transit intervals in the order of milliseconds. [3]

Presently the only commercial supplier of this sort of system is STELAR SRL. It provides relaxometers that use MOSFET networks capable of the peak power needed (up to 15 kW [7]) for acceptable switching times. [5] The control system of this power supply is also based on feedback measurement of the magnet current, which is compared with a reference signal.

One solution developed by a DECC-IST/CFMC partnership considers a pulsed switched power supply, using power semiconductors in their saturation and cut-off states. The switching circuit is coupled to a DC power source of voltage U. The voltage applied to the coil U_M depends on the states of the power semiconductors and can assume values $(-U, 0, U)$. Depending on the reference current, the value of U_M changes so that the magnet current transits between high and low levels within milliseconds and the output current ripple during the steady state regimes is reduced to acceptable values. [8]

A more recent design of a FFC power supply uses recent IGBT semiconductors and a direct control of their gate voltage, which allows to regulate the magnet current within the limits of the FFC NMR specifications. [9] One

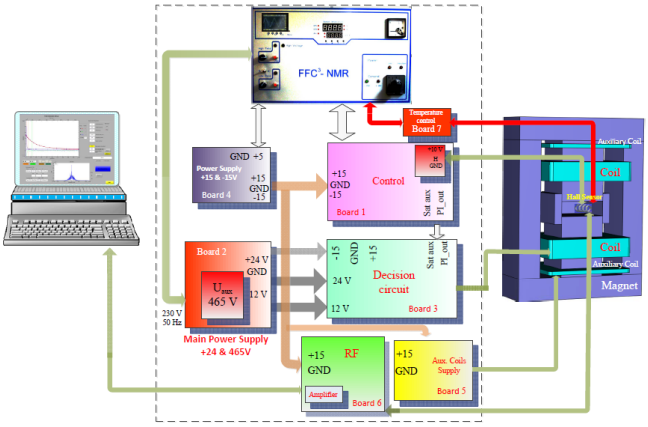

Figure 3: Architecture of a modern fast field cycling relaxometer (proposed by Roque et al [10]).

common aspect of the control units of the power supplies developed so far is the use of analog electronics in their implementation.

In this project a digital power control unit was developed and integrated in the power supply of a new relaxometer prototype under development. [10] The new FFC magnet under development has $R = 3\Omega$ and $L = 270\text{mH}$. The rather large inductance is due to the fact that it has a laminated iron core. One advantage of this type of FFC magnet is the fact that the currents required to produce a given magnetic field are lower than for an equivalent air-core magnet. The disadvantage is the rather large self-inductance in comparison with the air-core magnets. This solution uses an IGBT power semiconductor (IGBT-IXGH16N170), capable of controlling currents up to 32 A and offering a favorable DC current gain ($\beta = 700$). In this configuration direct measurements of the magnetic field strength are used as feedback to the control system. The magnet current is adjusted by direct control of the gate-emitter voltage. This is carried out by control electronics which compares the output voltage $U_{Hall}(t)$ of the *Hall* sensor placed near the sample with a reference signal $r(t)$.

The architecture of the relaxometer is presented in Figure 3.

A 24V DC Power Supply is used to excite the magnet coils. Fast switching from a lower current level to a current value corresponding to a high magnetic field strength is possible using a 500V DC auxiliary power supply. As the voltage applied to the coil increases, the rate of change of current also increases. Other power supply excites auxiliary coils which compensate the Earth magnetic field and the residual magnet's core field. An RF unit produces the detection pulse after an upward transition. An independent control unit maintains the desired sample temperature.

IGBT Gate-Emitter voltage is adjusted by the control system to obtain the magnet field required. This is accomplished by an analog PI control system which compares the output voltage from the *Hall* sensor and a voltage reference. In addiction, the control system turns on the auxiliary high voltage supply during the upward switching phase. The control unit receives two TTL pulses which command each transition (downward and upward) and a reference voltage from the NMR console. The control electronics output signals consist in

the IGBT gate voltage signal (PI_out) and a pulse signal (Sat_aux) that turns on the auxiliary power supply during the upward transitions.

The main goal of this project is to develop a more versatile and modular digital system which can replace the analog system solution for controlling the magnetic field of the new FFC-NMR relaxometer prototype under development. [10]

THEORETICAL BACKGROUND

NMR Relaxometry Theory

Nuclear Magnetic Resonance techniques are based on the interactions between nuclear spins in a system and a externally applied magnetic field $\boldsymbol{B_0}$.

When spins are exposed to an externally applied field B_0, the interaction between the magnetic moment μ and this field results in a splitting of the energy levels that are degenerate in the absence of the magnetic field. This interaction is called *Zeeman* Effect. [4] [11] Different spin states, that are degenerate in thermal equilibrium, have different energies in a non-zero magnetic field. For two adjacent levels, their energy differ by $|\Delta E| = \gamma\hbar B_0$. As a result, the frequency of radiation that induces a transition between adjacent levels is given by the *Bohr* relation

$$\omega_0 = 2\pi\frac{|\Delta E|}{h} = \gamma B_0 \tag{1}$$

ω_0 is the *Larmor* frequency and in a classical picture this frequency is the equivalent of the precessing frequency of a magnetic moment around the magnetic field axis. For the usual magnetic fields in a NMR laboratory, this $\omega_0/(2\pi)$ is in the radio-frequency range.

In a basic NMR experiment, starting from equilibrium in the presence of a *Zeeman* field $\mathbf{B}_0$, a spin system is irradiated with a radio frequency (rf) field $\boldsymbol{B}_1$, tuned in resonance with the *Larmor* frequency of the nuclear magnetic spins and orthogonal to the static field direction. In this process the system is disturbed from its initial state and starts returning to the equilibrium. [1]

There are two relaxation mechanisms that nuclear spins undergo starting from a non-equilibrium state. These mechanisms are related with the evolution of the different components of the net macroscopic magnetization $\mathbf{M}$ under the relaxation process.

Magnetization vector $\mathbf{M}$ is the vector sum of the contributions from each nuclear magnetic moment μ of the sample. Figure 4a represents an individual magnetic moment precessing around B_0, while figure 4b shows the net magnetization resulting from the precession of an ensemble of identical magnetic moments of nuclei with $I = 1/2$. At equilibrium, the net magnetization is given by the *Curie*'s law $M_z = \frac{n\gamma^2\hbar^2 S(S+1)}{3kT}B_0 = \chi B_0$.

In thermal equilibrium, the net macroscopic magnetization is oriented in the direction of the applied *Zeeman* field (conventionally oriented along the z axis) since there are more nuclei aligned with $\mathbf{B}_0$ than in any other possible state. Moreover, all moments precess around $\mathbf{B}_0$ at the same frequency ω_0. Consequently, there is no phase coherence of the nuclear spins in the transverse plane and, therefore, magnetization xy-components are zero. [11]

Once a radio-frequency field perturbs the equilibrium state, the net macroscopic magnetization $\boldsymbol{M}$ change and, after the perturbation, each component undergo in a relaxation process returning to the thermal equilibrium. The magnetic vector of the rf field $\boldsymbol{B}_1$ can be seen as a field rotating in the xy-plane at angular frequency ω_0, represented in 4a. [11]

In *spin-lattice* or *longitudinal* relaxation process, the nuclear spins exchange energy with their surroundings, the *lattice*, allowing the spin populations to return to the equilibrium. This process brings the z-component of the magnetization vector $\boldsymbol{M}$ to its thermal equilibrium value M_{zeq} with a time constant denoted by T_1.

Another relaxation process is related with the fading out of phase coherence in the transverse plane. As discussed earlier, in equilibrium state the xy-components of the magnetization vector are zero. However, when a radio-frequency field on resonance disturbs the equilibrium, phase coherence is created in the transverse plane. The transverse components of the vector $\boldsymbol{M}$ return to zero after the perturbation, as the phase coherence in the xy-plane disappears. The time constant for this process is denoted by T_2 and corresponds to the decay constant of the *transverse* or *spin-spin* relaxation, which involves energy exchange between spins resulting from magnetic dipole-dipole interactions in the system.

The behavior of the net magnetization during the relaxation process is well described by the *Bloch* equations 4 referred to a coordinate system (x', y', z') with $z' \equiv z$, which rotates about the static field $\boldsymbol{B}_0$ in the same direction which the nuclear moments precess. [4] If this frame of reference rotates with an angular frequency corresponding to the *Larmor* frequency of this precession motion and assuming there's no longer the rf field perturbation, then the *Bloch* equations for the relaxation process of the net macroscopic magnetization are simply:

$$\frac{\mathrm{d}\,M_{x'}(t)}{\mathrm{d}t} = -\frac{M_{x'}(t)}{T_2} \tag{2}$$

$$\frac{\mathrm{d}\,M_{y'}(t)}{\mathrm{d}t} = -\frac{M_{y'}(t)}{T_2} \tag{3}$$

$$\frac{\mathrm{d}\,M_z(t)}{\mathrm{d}t} = -\frac{M_z(t) - M_{eq}}{T_1} \tag{4}$$

Since $\boldsymbol{B}_1$ rotates at the same frequency as the frame, $\boldsymbol{B}_1$ can be arbitrarily aligned along the rotating axis x'. When the rf field is applied, the net magnetization precess about $\boldsymbol{B}_1$ in the rotating frame at a frequency given by the *Larmor* condition $\omega_1 = \gamma B_1$, as is showed in 5a. Usually, a radio frequency pulse is applied in a coil during a period of time t_p, in the order of microseconds, causing the net magnetization to flip around the x' axis by an angle $\phi = \gamma B_1 t_{pulse}$. [11]

After being tipped through an angle ϕ about B_1 (figure 5a), the net magnetization presents a component along y'. Due to energy exchange between the nuclei, $M_{y'}$ decays with a time constant T_2 (figures 5b and 5c). *Spin-lattice* relaxation also occurs as the nuclear spin system loses energy to its surroundings and $M_{z'}$ returns to its equilibrium value M_{eq} with a time constant T_1 (figure 5d).

Radio Frequency pulses and FID

The determination of T_1 and T_2 implies evaluating the magnitude of the different components of the net magnetization vector $\boldsymbol{M}$ during the relaxation process. This is

Figure 4: **(*a*)** Precession of a magnetic moment $\boldsymbol{\mu}$ in the presence of a magnetic field $\boldsymbol{B_0}$. epresentation of the rf field $\boldsymbol{B_1}$ component rotating in the xy plane in resonance with the *Larmor* frequency. **(*b*)** Net macroscopic magnetization vector resulting from the precession of an ensemble of identical magnetic moments of nuclei with $I = 1/2$.

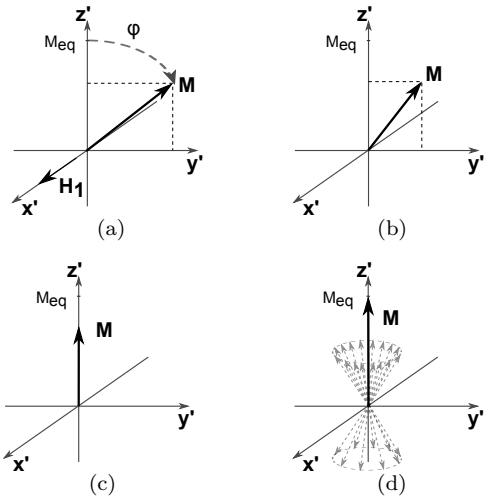

Figure 5: Evolution of the net macroscopic magnetization in the rotating frame after being tipped through an angle ϕ.

accomplished by measuring the signal induced by $\boldsymbol{M}$ in a coil along a fixed axis transverse to the *Zeeman* field $\boldsymbol{B}_0$. This signal is called Free Induction Decay (FID) and is detected after applying a proper rf pulse, which causes $\boldsymbol{M}$ to spiral around B_0 until it makes angle $\phi = \gamma B_1 t_{pulse}$ with respect to B_0. The $M_\perp$ component of the magnetization precesses then freely around B_0 with decreasing amplitude and induces in the coil an electromotive force according with the Faraday's induction law. The magnitude of $\boldsymbol{M}$ along the coil axis determines the strength of the observed signal, and, as the relaxation processes occur, the signal decays. [1]

By measuring the magnitude of the net magnetization components for different instances during the relaxation process, we can estimate the relaxation time constants.

Fast Field Cycling NMR

Standard NMR techniques apply different rf pulse sequences to measure the net magnetization components at distinct times, having the sample under the influence of a constant field $\boldsymbol{B}_0$. On the other hand, the FFC experiments consist in cycling the *Zeeman* field, as represented in Figure 6.

The cycle starts after a polarization time t_P, where the sample is subjected to a field $\boldsymbol{B}_{0P}$ as high as possible for a given equipment. The magnetic field is then switched down to a lower value in a short time t_{off}, after which the spin system relaxes towards the new equilibrium situation corresponding to the value $\boldsymbol{B}_{0E}$. The magnetization will then have a new value M_E, given by the *Curie*'s law. This relaxation process takes place in a low field time t_E. Both the length of the evolution time and the value of the field $\boldsymbol{B}_{0E}$ are adjustable. Finally, the signal remaining after the evolution period is detected in a high field $\boldsymbol{B}_{0D}$. Again, during the detection time t_D the intensity of the induction is increased as far as practicable. The FID signal is obtained by a standard application of a rf pulse in resonance with the *Larmor* frequency $\omega_{0D} = \gamma B_{0D}$. In a typical experiment, the cycle of period T is followed by an extended delay for the restoration of the thermal equilibrium and polarization. This procedure is repeated many times with different lengths of t_E to observe the behavior of the spin system and to perform relaxation measurements. [3]

The spin-lattice relaxation process occurring during the evolution period is governed the *Bloch* equation 4. A proper integration gives the behavior of the longitudinal component of the net magnetization through out t_E.

$$M_z(t) = M_{eq}(B_{0E}) + [M_z(t_E = 0) - M_{eq}(B_{0E})] \exp\left(-\frac{t}{T_1(B_E)}\right) \quad (5)$$

In the initial period of polarization, it is expected that M_z reaches the equilibrium value $M_P \equiv M_{eq}(B_{0P})$. A downward transition to a selected level B_{0E} in a time much shorter than t_E allows the relaxation of the magnetization towards a new equilibrium $M_E \equiv M_{eq}(B_{0E})$ (Figure 6). Finally the magnetic field is switched up to a a higher magnetic field so that the detection of the NMR signal can be made with a reasonable SNR.

The behavior of M_z as a function of t_E can be detected by means of a rf field $\boldsymbol{B}_1(t)$ applied in resonance with the Larmor frequency $\omega_{0D} = \gamma B_{0D}$, which flips $\boldsymbol{M}_z(t = t_E)$ by an angle of $\pi/2$. This pulse is applied after the upward switch to the detection field and after a stabilization delay. The detection of the FID is made exactly as in the case of conventional relaxometry. This gives rise to a typical FID signal in a coil placed around the sample.[3] [11] The initial height of the FID signal is proportional to the magnetization $M_z(t = t_E)$. If this measurement is repeated for different lengths of t_E, the relaxation time constant T_1 associated to the low field $\boldsymbol{B}_{0E}$ can be determined by fitting the measured data with equation 5 (see Figure 6). [3] [5]

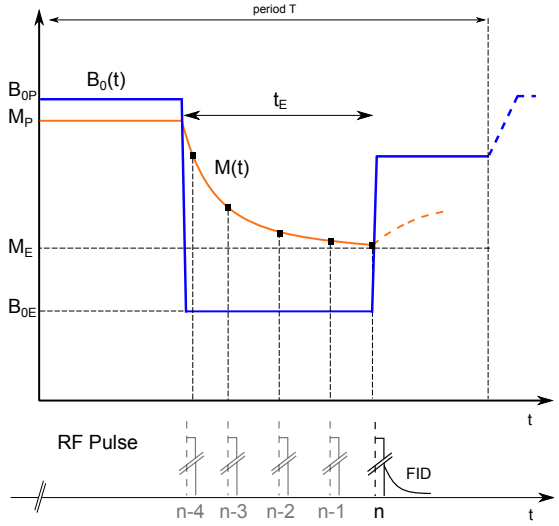

Figure 6: *Zeeman* field cycle with the representation of the measurements for different lengths of t_E.

Signal Sensitivity in NMR and Field Cycling Requirements

NMR relaxometry at low frequencies is practically impossible using standard techniques with a constant *Zeeman* field. Low-frequency studies imply decreasing the field strength due to the *Larmor* condition. Since the NMR induction signal weakens as B_0 decreases, for a field strength smaller than 0.09T, this usual approach becomes more and more difficult to perform.

The signal-to-noise ratio in NMR experiments follows [2] [3] SNR $\propto B_0^{3/2}$. Clearly the FFC technique makes possible to overcome this difficulty for low magnetic fields (low frequencies), since the detection is made at a fixed frequency, independent of the value of the magnetic field (frequency) at which the $M_z\,(t_e)$ is studied. Therefore the measurement of $T_1\,(B_e)$ is made always with a reasonable SNR.

Ideally, FFC experiments eliminates sensitivity problems related to low frequency measurements. Moreover, since the NMR signal detection occurs at one single field ($\boldsymbol{B}_{0D}$), the *Larmor* frequency in study can be changed (altering the field strength $\boldsymbol{B}_{0E}$) without the necessity to retune the spectrometer.

All these characteristics make FFC-NMR a powerful and versatile technique, that enables molecular dynamic studies in several time scales, being less time consuming than other common procedures.

To perform a reasonable FFC-NMR study, the *Zeeman* field modulation has to fulfill some requirements through out the different phases of the field cycle. Nevertheless, the field modulation should ensure the cycle to be reversible. In other words, the field cycle is reversible if the order of the nuclear spins can follow the reorientation of the *Zeeman* field. [3] [5]

For the cycle to be reversible, sufficiently homogeneous and stable magnetic inductions must be produced during the stationary phases, namely during the polarization, evolution and detection periods. During t_P and t_D, the field should be as high as possible, but a stable and homogeneous field during these periods is crucial to allow NMR signal detection. Local field variations could lead to the appearance of phase coherence of the magnetic moments, creating transverse components of the net magnetization. Hence we would find a reduced projection along the *Zeeman* field due to magnetic field instabilities, which may compromise the measurements. However, from an experimental point of view, the critical phases of the modulation are the intervals (t_{off} and t_{on}) necessary to switch $\boldsymbol{B}_0$ between the selected upper and lower level with high accuracy. Both turn-on and turn-off must be fast enough when compared with relaxation time constants of the spin system to avoid energy transfer in these intervals. That is, the field control must be performed with a time resolution better than the shortest relaxation time to be expected for the samples under consideration:

$$t_{off} + t_{on} << T_1\,(\boldsymbol{B})_{min} \tag{6}$$

Here $\boldsymbol{B} = \boldsymbol{B}_0 + \boldsymbol{B}_{loc}$ is the total flux density 'seen' by the nuclei. $\boldsymbol{B}_{loc}$ corresponds to the internal magnetic field due to the presence of all other local permanent or induced magnetic moments (nuclear, atomic and/or molecular). The directions of the local fields are randomly distributed and do not coincide with that of the external magnetic flux density $\boldsymbol{B}_0$.

At high external magnetic inductions, $B_0 >> B_{loc}$, the local fields can be neglected and the spin orientations follow the direction of $\boldsymbol{B}_0$. In the case of low external fields such that $B_0 \approx B_{loc}$, a well defined orientation of the spin system is maintained as long as the effective field $\boldsymbol{B}$ does not fluctuate non-adiabatically in time. The adiabatic condition for $\mathrm{d}\boldsymbol{B}/\mathrm{d}t$ is written in the form

$$\left|\boldsymbol{B} \times \frac{\mathrm{d}\boldsymbol{B}}{\mathrm{d}t}\right| / B^2 << \gamma B \tag{7}$$

This means that the field transitions should be slow enough compared with the *Larmor* period, so that $\boldsymbol{M}$ can follow the reorientation of the effective field, preserving the angle between $\boldsymbol{M}\,(t)$ and $\boldsymbol{B}\,(t)$. [3] [5]

FFC NMR RELAXOMETER PROTOTYPE

The magnet current of the FFC relaxometer has to be controlled so that the *Zeeman* field generated switches between low and high levels as required by this NMR technique.

In this project, a ferromagnetic-core magnet with inductance L_M and internal resistance R_M is excited by two power sources (U_0 and U_{aux}).

The main power supply control system of the FFC relaxometer is represented in Figure 7. A 24V DC power supply (U_0) feeds the magnet through the cycle. A high voltage auxiliary power supply (U_{aux} = 500V DC) is turned on by the control system only during the upward transition, making possible to obtain short switching times from a low relaxation level to the high polarization magnetic field. An IGBT device is used to control the magnet current. A resistance R_E is included between the IGBT emitter and ground. Comparing the *Hall* sensor output voltage $u_{Hall}\,(t)$ with a reference signal $r\,(t)$, control electronics adjusts the gate-emitter voltage v_{GE} through the command signal $u_C\,(t)$ in order to reach the current level necessary to generate a magnetic field strength B_0 corresponding to the reference imposed.

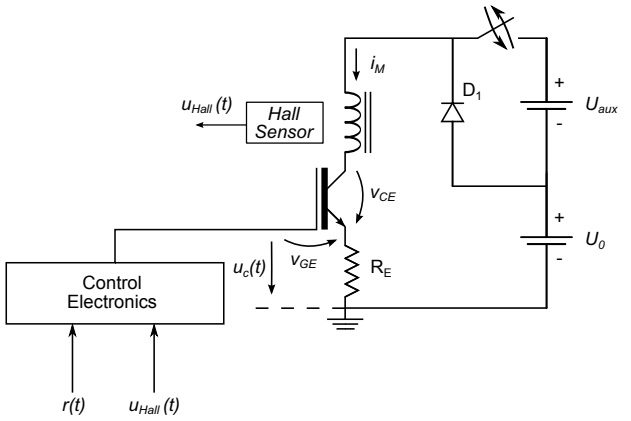

Figure 7: Main power supply control circuit of the FFC relaxometer.

When the auxiliary voltage supply is turned off, the circuit voltage balance is given by

$$\frac{\mathrm{d}i_M}{\mathrm{d}t} = \frac{1}{L_M}\left(U_0 - v_{CE}\right) - \frac{i_M}{\tau_L} \tag{8}$$

where $\tau_L = L_M/\left(R_E + R_M\right)$.

An incremental change in the gate-emitter voltage results in a change in the collector current and since

$$\Delta v_{CE} = \beta\left(R_E \Delta i_M - \Delta u_C\right) \tag{9}$$

the magnet current can be adjusted by changing the gate voltage command u_C.

The transitions between magnet current levels have to be fast, but should be long enough so that the net magnetization follows the *Zeeman* field reorganization. Clearly, these limits depend upon the spin system in consideration. Thus, in terms of technical realization, transition times in the order of milliseconds ($\approx 3\,\mathrm{ms}$) are acceptable for most soft materials ([12] [2]).

To reach a switching time in the order of milliseconds in an upward transition, an auxiliary power supply is used. The control electronics transfers the IGBT transistor to saturation as the magnet current rises, reaching its steady state value.

An analogue PI controller can be used to control the *Zeeman* field in FFC experiments. This controller adjusts the IGBT gate voltage $u_C(t)$ so that the error difference between the *Hall* sensor output $u_{Hall}(t)$ and the reference signal $r(t)$ is minimized. The output $u_c(t)$ is the result of the sum of two correcting terms:

$$u_c = k_P\left[e(t) + \frac{1}{T_I}\int_0^t e(\tau)\,\mathrm{d}\tau\right] \tag{10}$$

where k_P is the proportional gain, T_I is the integral time and

$$e(t) = r(t) - u_{Hall}(t) \tag{11}$$

The integral gain is determined by $k_I = \frac{k_P}{T_I}$. [13]

An analogue implementation has been used for this controller. It is able to produce fast switching of the magnetic field [10] This project aims to develop a digital PID controller which can replace the analog version. The main goal is to turn the control of the relaxometer power supply more flexible. Assuming that suitable programming tools are available, it is generally much easier to change the specifications of a digital control loop than to change the physical parameters of its analogue counterpart. The implementation of a digital controller will allow to span the number of many alternatives in terms of the Fast Field Cycling specifications. In the first instance, changeable switching times and applying different field sequences are two of the most promising enhancements that will be possible using a digital controller and that are much harder (or even unpractical) to implement in the analogue version.

DIGITAL PID CONTROL

Concerning a digital version of a PID controller, a discrete algorithm has to be implemented. Let's consider the continuous time expression of an ideal PID controller [14][15]:

$$u(t) = K_p \times \left[e(t) + \frac{1}{T_I}\int_0^t e(\tau)\,\mathrm{d}\tau + T_D\frac{\mathrm{d}}{\mathrm{d}t}e(t)\right] \tag{12}$$

Using finite differences approximations on the continuous time expression of a PID controller (Equation 12), a discrete time PID control law can be expressed as the following equation:

$$\begin{aligned} u(t_k) = u(t_{k-1}) + K_p\left(e(t_k) - e(t_{k-1})\right) + K_i\left(e(t_k)\right) \\ + K_d\left(e(t_k) - 2e(t_{k-1}) + e(t_{k-2})\right) \end{aligned} \tag{13}$$

Equation 13 is the *Velocity Algorithm* for a PID controller [14][15], derived by approximating the first-order derivatives via backward finite differences, where control parameters are treated as simple gains ($K_i = \frac{K_p}{T_i}$ and $K_d = K_p T_d$).

Digital Control System

The digital control system for a FFC power supply has to fulfill the following requirements:

- to read the feedback measurements from the *Hall* sensor;
- to detect TTL pulse signals ($0-5$ V square wave) that command the field transitions;
- to send a pulse signal to turn on the auxiliary power supply during the upward transition;
- and to produce the IGBT gate command signal, resulting from control operations.

In this project, a *digital signal controller* (Microchip ®dsPIC30F4013) is used to implement the PID controller. This processing unit incorporates several useful peripheral components, including 5 timers ($16-$bit resolution), $12-$bit Analog-to-Digital Converter and an Output Compare Module. For example, the Analogue-to-Digital Converter is used to acquire the *Hall* sensor output voltage. On the other hand, the dsPIC30F4013 does not incorporate a Digital-to-Analogue converter necessary to generate the analogue output signal to command the IGBT. Therefore, a Pulse Width Modulation (PWM) DAC will be implemented to overcome this issue.

However, this solution involves analog low-pass filtering the PWM signal to remove high frequency components. Therefore, the control variable is the PWM duty cycle and the analog output signal corresponds to a fraction of the pulse voltage.

The different input and output signals of the digital control system are represented in Figure 8. In this control system, the reference signal $r(t)$ is a digital value that has to be predetermined in the system initial configuration. Once a transition is commanded through one of the TTL pulses, the control reference value changes accordingly. Following an upward command pulse, the controller turns on the auxiliary voltage supply and drives the IGBT semiconductor to saturation. When the *Hall* sensor output voltage is near the reference value, the auxiliary voltage supply is turned off and PID calculations have to adjust the IGBT gate voltage, in order to minimize the error difference between the *Hall* sensor feedback signal and the field reference value. Once a downward command pulse is detected, the controller imposes a low voltage on the IGBT gate to obtain a fast downward transition. The PID controls the stability of the field on a low reference value.

Control Operations

Generally speaking, a digital PID controller operates continuously reading signals from sensors, sampling and converting them to digital form by means of a analog-to-digital convertor. The control signal must be computed and then converted to analog form for the actuators. A typical operation sequence is as follows: [16]

1. Wait for a clock interrupt.
2. Read input from sensor.
3. Compute control signal.
4. Update controller variables.
5. Send output to the actuator.
6. Repeat from 1.

The computation of the controller parameters must occur out of the main loop, to minimize the time delay.
The relaxometer power supply control system is implemented as a embedded application based on on-chip peripheral interrupts that initiate processes on CPU to deal with the events. For example, when an A/D conversion is completed, a signal is sent to the processor indicating this event occurred, requiring the interruption of the current code the processor is executing. A timer is used to start the sampling and A/D conversion process at a desired frequency (25kHz). The change of state on specific input ports (RB4 and RB5) determines the instant of upward and downward transitions, respectively. When a TTL pulse is detected on the input ports RB4 or RB5, a Change Notification interrupt request is generated. In this interrupt handler the I/O ports are read, determining which pin was driven high. If PORTBbits.RB4 = 1, an upward transition has been commanded and the RB6 pin is driven high, switching on the auxiliary power supply. The field reference is set as a value corresponding to a high magnetic field. If PORTBbits.RB5 = 1, a downward transition has been commanded and the control system output is set to a low constant value. The field reference changes to a low magnetic field value.

A transition to a high polarization field is dictated by a TTL pulse which originates a change of state on input port RB4. Change Notification ISR is executed and determines which is the digital reference value that is used in the control loop, by setting the value of y. When RB4 pin is driven high (reading PORTBbits.RB4 = 1), its value is set to $y = 1$.

Variable y determines not only which control reference value is used, but also the PID parameters in the control calculations. CN ISR starts Timer5 and RB6 pin is driven high, leading the IGBT to the saturation region and turning on the auxiliar voltage supply. This way a transition to a high polarization field can be accomplished within milliseconds.

Timer5 is used to limit the time period the high voltage is applied on the coils excitation avoiding IGBT damage, during the upward transition.

Timer4 interrupt is requested at 25 kHz and sets A/D Sample Enable bit. In other words, A/D sampling is enabled in the Timer4 ISR and the start of the conversion is right after the sampling period. Therefore, for each Timer4 interrupt, there's an A/D sample and conversion of the analogue signal from the Hall Sensor , followed by an A/D Conversion Complete ISR request to the processor. This interrupt handler compares the result of the A/D conversion to a reference value corresponding to a high magnetic field. PID control of the IGBT voltage gate starts when the control error is less than a threshold value ϵ_2. Otherwise, the control system output is maintained as a high value. Consequently, the PWM duty cycle is near 100% in the first control cycles during the upward transition.

Once the Error is less than ϵ_2, RB6 pin is driven low, turning off the auxiliar voltage supply, and, from this point on, PID calculations are taken into account and the control system output (i.e. the PWM duty cycle) is the result of the function PID algorithm.

From the moment the high voltage supply is turned off, the control action is the result of the PID calcultions. The control signal is formed from the error between the field reference and the digital value returned by the ADC module, corresponding to the last measurement of the Hall sensor analogue signal. PID controller is responsible for the adjustment of the PWM duty cycle. This action on the IGBT gate voltage must guarantee a fast-settling time, after an upward field transition.

A transition to a low relaxation field is dictated by a TTL pulse, detected on pin RB5. A change of state on RB5 (reading PORTBbits.RB5 = 1) originates a Change Notification interrupt request to the processor. In the interrupt handler, variable y is set as -1 and a constant low value is kept as the control output.

From the instant the processor executes the CN ISR, every single ADC measurement of the Hall sensor signal is compared to a low field reference value in the ADC interrupt handler.

If the value read from the Hall sensor is far from the low reference value, then in the control output is kept a constant low value, allowing a fast downward field transition. For this reason, in the first control cycles of the

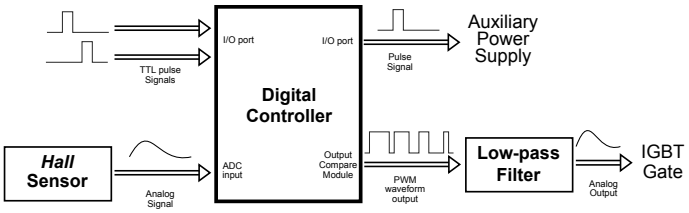

Figure 8: Digital control system input and output signals.

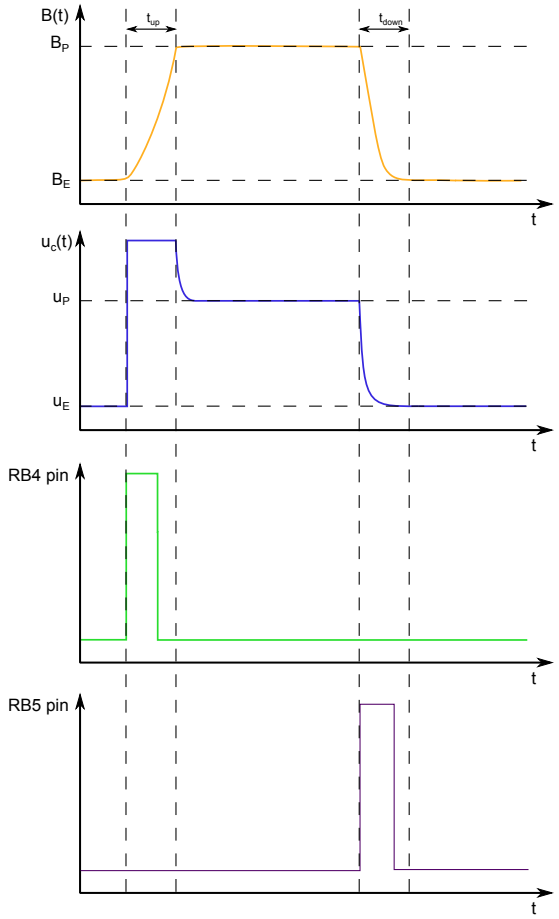

Figure 9: Field cycling sequence. Shown are the magnetic flux density $B\,(t)$, the IGBT gate voltage $u_c\,(t)$ and the states on RB4 and RB5 pins.

transition to a low relaxation field, the PWM duty cycle is constant and near the minimum value allowed in the IGBT conduction state.

Once the error is smaller than a threshold value ϵ_1, PID controller starts adjusting the PWM duty cycle, in order to settle the field on its final value.

After the downward transition, the control signal is formed from the error between the field reference and the digital value returned by the ADC module, corresponding to the last measurement of the Hall sensor analogue signal. PID controller action on the IGBT gate voltage must guarantee a fast-settling time, after a downward field transition.

EXPERIMENTAL SETUP

Figure 10 shows a conceptual scheme of the control system, with different conditioning stages and low pass filters necessary for this application.

First, a low-pass filter is used in the conversion of the PWM waveform to an analog signal, followed by a conditioning stage, where amplification of the signal is done in such a way that it meets the requirements of the plant (IGBT gate). A *Bessel* low-pass filter was designed with a cutoff frequency of $f_c = 2.5\,\text{kHz}$ for this purpose. On the other hand, an anti-alias low pass filter and a conditioning stage are placed between the Hall sensor and the A/D converter. This low-pass filter is required to reduce the higher-frequency noise components in the analog signal. Noise components with a frequency much higher than the control system bandwidth can be aliased down so that the closed-loop system respond to noise.

EXPERIMENTAL RESULTS

The digital controller was tested as the main controller of the magnetic field produced by the magnet of a pre-production prototype NMR relaxometer.

Different sets of PID parameters were experimentally tested to obtain fast adiabatic field transitions to perform spin-lattice relaxation measurements. As explained earlier, upward and downward magnetic field transits should be fast enough when compared with the relaxation time constants of the spin system to reduce as much as possible the energy transfer during these intervals. On the other hand, the transitions should be slow enough in order to maintain the alignment of the magnetization and avoid any transverse component. Both conditions depend on the sample in study, but in terms of technical realization, the upward and downward switching times should be in the order of milliseconds ($t_{on}, t_{off} \approx 3\text{ms}$).

In Figure 11 is presented the evolution of the PWM waveform and magnetic field during a downward transition between the high polarization field and a low relaxation field.

As expected, the controller adjusts the PWM duty cycle so that the magnet current level varies in order to minimize the error between the digital reference and the *Hall* sensor feedback voltage. Figure 11 corresponds to the time instant that a downward transition is triggered and the digital reference of the controller changes to a predetermine lower value. PWM duty cycle is immediately reduced, stabilizing in a lower value corresponding to the IGBT gate voltage required so that the magnetic field strength reaches the reference value.

Several sets of PID parameters were tested on the control system. Table I presents the PID controller parameters for the upward and downward transitions. These parameters allowed to obtain fast and smooth transit regimes, without under or overshooting the magnetic field strength values in the steady state regimes as showed in Figure 12.

The ripple voltage observed on the IGBT gate, due to low-pass filtering the PWM signal, does not seem to

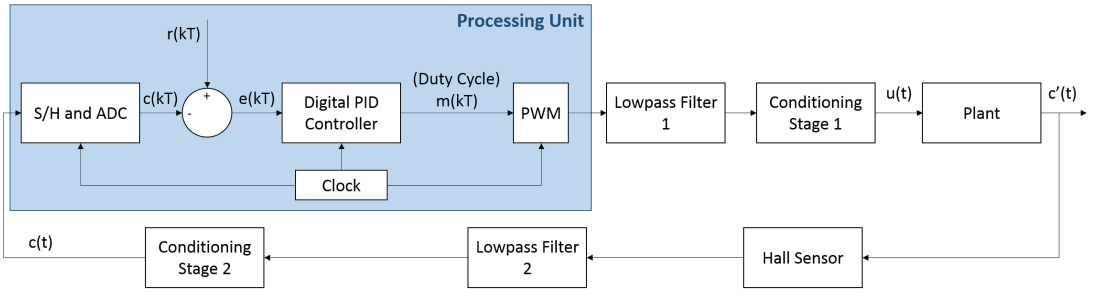

Figure 10: Conceptual scheme simplified of the control system implemented.

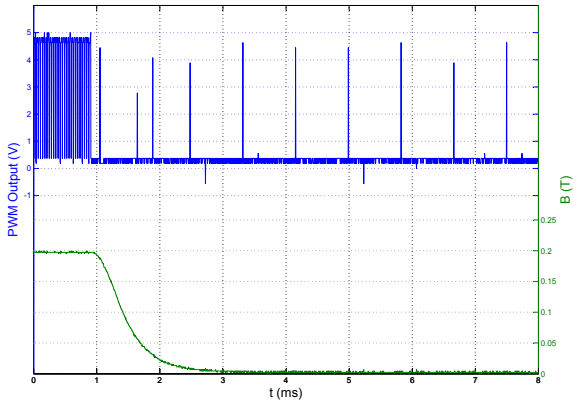

Figure 11: Magnetic field strength and PWM waveform during a downward transition.

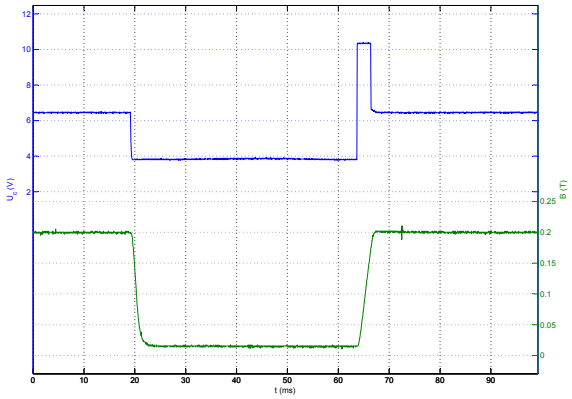

Figure 12: IGBT gate voltage and B_0 in a complete field cycle.

PID Parameters	Upward Transition	Downward Transition
k_P	2800	3000
k_I	33	20
k_D	0	0

Table I: PID parameter sets used for controlling the upward and downward transitions.

Sample	f (kHz)	Digital Control		Analog Control	
		T (°C)	T_1 (ms)	T (°C)	T_1 (ms)
5CB	300	26.0	43.4 ± 4.3	25.0	42.9 ± 4.3
	300	26.0	46.6 ± 4.7	25.8	42.5 ± 4.3
	1000	20.0	40.8 ± 4.1	23.8	48.6 ± 4.9
	1000	26.0	59.2 ± 5.9	24.2	49.8 ± 5.0
[BMIM]BF4	300	26.0	80.3 ± 8.0	26.4	78.6 ± 7.9

Table II: Results of the spin-lattice relaxation time measurements using digital and analog control systems.

perturb significantly the magnetic field strength stability. However, the relevance of this variation can only be tested observing the NMR signal quality.

In order to assess the digital control system performance, measurements of the proton spin–lattice relaxation time T_1 of two distinct samples were realized using the developed solution to control the magnet current. These experiments were performed with the liquid crystal 5CB and the ionic liquid compound [BMIM]BF4. The liquid crystal 5CB is commonly used as a reference for testing and comparing the performance of relaxometer experimental setups. [8] The ionic liquid was used because it's one of the systems recently studied using the previous generation of FFC relaxometer.

The FFC-NMR measurements quality depends on many factors other than the control system efficiency. A good adjustment of all the system components is crucial for the FID signal and, overall, the FFC-NMR measurements quality. Therefore, measurements under the same conditions were performed with the same relaxometer, although using the analog control system of the power supply. Table II compares the results obtained with each control system for a better assessment of the digital system performance.

The analysis of the spin-lattice relaxation time measurements obtained with each control system shows that the digital control system allowed to obtain results in the same order of magnitude as the measurements performed with the analog controller.

On the other hand, in the case of the 5CB liquid crystal, it could be argued that there are greater discrepancies between measurements at the same frequency obtained with the digital control system than with the analog controller. These discrepancies could be a consequence of a deviation from resonance, due to magnetic field instabilities during the steady state regimes. These instabilities can produce transverse nuclear magnetization, lowering the magnitude measured which should be the result of the longitudinal relaxation process only. The transition

periods can also contribute for these variations of the T_1 measurements. If the magnetic field does not reach and settle at its final value within 3 ms in each transition, the reproducibility of the measurements may be compromised. This could explain the 5CB liquid crystal measurements at 1MHz obtained using the digital controller, which differ almost 20 ms. However, these results have to be interpreted with caution, since the relaxation time constant T_1 depends on the temperature of the sample and these measurements were performed at $20°C$ and $26°C$, respectively. Besides, all the experimental results for 5CB liquid crystal at a frequency of 300 kHz (including the measurements using the analog controller) were obtained at a temperature within the range of 25 to $26°C$. These results are compatible within the experimental error suggesting that the digital system can provide the magnetic field control as efficient as the analog implementation.

The experimental results obtained for the ionic liquid compound [BMIM]BF4 at a frequency of 300 kHz using the analog and digital controllers are also quite consistent, suggesting likewise that the digital system developed modulates the *Zeeman* Field as required in an FFC-NMR experiment.

CONCLUSIONS

Fast Field Cycling Nuclear Magnetic Resonance is a powerful technique which makes possible to perform spin-lattice relaxation studies in a broad frequency range. This technique involves having the sample in different fields B_0 at different times, which allows to measure the relaxation time T_1 related to a low field B_E with a NMR signal sensitivity of a common high field measurement. This technique can be very demanding from the point of view of experimental equipment. It requires that the magnetic field cycles between homogeneous, steady-state regimes, with switching times within $1 - 3$ ms for most experiments with soft materials.

The main purpose of this project was to develop a digital control system capable of modulating the *Zeeman* field of a FFC-NMR relaxometer under development at Instituto Superior Técnico. In order to modulate the magnetic field, the magnet current is controlled using an IGBT device.

This was accomplished by configuring and programming a Microchip® dsPIC microcontroller and implementing some additional filters and driving on-chip peripherals to interface with sensors and power electronic devices. The program developed configures the MCU core and several peripherals required for the application. The sequence of control operation starts with a timer interrupt, enabling the Analog-to-Digital conversion of the signal from the Hall sensor placed near the sample inside the magnet. The result of this conversion is compared with a predetermined digital reference. The error difference between these two values is then minimized as the PID algorithm adjusts the control system output.

The result of the control operations corresponds to the duty cycle of a PWM waveform generated by a dsPIC peripheral. A *Bessel* low-pass filter converts this signal to an analog voltage that regulates the magnet current through the IGBT gate. Thus, the magnetic induction produced in the magnet reaches the corresponding control reference value.

The transitions between low and high current levels are triggered by TTL pulses detected at specific input ports of the microcontroller. The control system is responsible for turning on an auxiliary power supply only during the upward transitions.

The software and hardware were designed to allow fast transitions as required in a FFC-NMR measurement. The experimental results show that transitions between the high polarization field and a low relaxation field are successfully realized within milliseconds.

Furthermore, the digital system developed was used to modulate the *Zeeman* field while measuring the spin-lattice relaxation time T_1 of the liquid crystal 5CB and the ionic liquid [BMIM]BF4 for two different relaxation fields. The exponential decay of the nuclear magnetization was observed and the related time constant was determined for each case. Results suggest that the control system designed in this work can be integrated in the relaxometer power supply system.

[1] M. Levitt, *Spin Dynamics: Basics of Nuclear Magnetic Resonance* (Wiley, 2001).

[2] D. de Mesquita e Sousa, *Desenvolvimento de um espectrómetro de ressonância magnética nuclear de campo cíclico rápido*, Master's thesis, Instituto Superior Técnico (2003).

[3] F. Noack, *NMR Field-cycling Spectroscopy: Principles and Applications*, Progress in nuclear magnetic resonance spectroscopy (Pergamon, 1986).

[4] T. Farrar and E. Becker, *Pulse and Fourier transform NMR: introduction to theory and methods* (Academic Press, 1971).

[5] E. A. Rainer Kimmich, Prog. Nucl. Magn. Reson. Spectrosc. **Volume 44**, 257 (2004).

[6] J. S. F. NOACK, St. BECKER, Annu. Rep. NMR Spectrosc. **33**, 1, 36 (1997).

[7] *Spinmaster FFC - 2000, Fast Field Cycling NMR Relaxometer Reference Manual*, STELAR s.r.l. (2001).

[8] D. Sousa, P. A. L. Fernandes, G. D. Marques, A. Ribeiro, and P. Sebastiao, Solid State Nucl. Magn. Reson. **25**, 160,166 (2004).

[9] D. de Mesquita e Sousa, G. D. Marques, P. J. O. Sebastiao, and J. M. B. Cascais, Solid State Nuclear Magnetic Resonance 1, **38**, 36 (2010).

[10] A. Roque, D. Sousa, E. Margato, and J. Maia, in *Power Electronics and Applications (EPE), 2013 15th European Conference on* (2013) pp. 1–9.

[11] N. Jacobsen, *NMR Spectroscopy Explained: Simplified Theory, Applications and Examples for Organic Chemistry and Structural Biology* (Wiley, 2007).

[12] D. Sousa, G. D. Marques, P. Sebastiao, and A. Ribeiro, Review of Scientific Instruments **74**, 4521 (2003).

[13] G. Franklin, J. Powell, and A. Emami-Naeini, *Feedback Control of Dynamic Systems* (Pearson Education, 2011).

[14] B. Liptak, *Instrument Engineers' Handbook, Fourth Edition, Volume One: Process Measurement and Analysis*, Instrument Engineers' Handbook (Taylor & Francis, 2003).

[15] K. Ogata, *Modern Control Engineering*, Instrumentation and controls series (Prentice Hall, 2010).

[16] K. Aström and R. Murray, *Feedback Systems: An Introduction for Scientists and Engineers* (Princeton University Press, 2010).